Macromolecules

ARTICLE

pubs.acs.org/Macromolecules

Mechanical Properties of Adhesive Films Obtained from PU−Acrylic Hybrid Particles

Elise Degrandi-Contraires,[†,#] Ravindra Udagama,[‡] Elodie Bourgeat-Lami,[‡] Timothy McKenna,[‡] Keltoum Ouzineb,[§] and Costantino Creton[*,†]

[†]Laboratoire de Physico-Chimie des Polymères et Milieux Dispersés, CNRS-UPMC-ESPCI Paristech, 10 rue Vauquelin, 75231 Paris cedex 05, France

[‡]Laboratoire de Chimie, Catalyse, Polymères et Procédés (C2P2), LCPP group, Université de Lyon, Univ. Lyon 1, CPE Lyon, CNRS UMR 5265, 43 Bd du 11 Novembre 1918, F-69616, Villeurbanne, France

[§]Research and Technology, Cytec Surface Specialties, Anderlecht Street 33, 1620 Drogenbos, Belgium

ABSTRACT: The mechanical and adhesive properties of films made from novel hybrid urethane/acrylic dispersions have been investigated. The adhesive films were obtained from the drying of bicomponent acrylic urethane latexes prepared by miniemulsion polymerization. In the companion paper, phase separation at the macroscopic scale was avoided by using a NCO end-functionalized polyurethane (PU) prepolymer and a hydroxyethyl methacrylate (HEMA) reactive comonomer in the acrylic backbone. The effect of two compositional parameters on the mechanical and adhesive properties was specifically studied: the PU weight fraction and the degree of grafting of the PU prepolymer on the acrylic backbone, controlled by the ratio between grafting agent HEMA and chain extender Bisphenol A (BPA). Swelling, rheological, tensile, and probe tack tests were used in parallel with an analysis of the macroscopic adhesive properties of the films. Results show that the PU weight fraction modifies significantly the small-strain elastic modulus and the gel fraction in the latex particle while the ratio HEMA/BPA can be used to adjust the chain length of the PU incorporated in the network. This ratio affects significantly the finite extensibility of the PSA while causing only relatively small changes in the low strain elastic modulus and gel fraction. An increase in the degree of grafting at fixed PU content is found to improve the resistance to shear of the adhesive without reducing its adhesion energy in a peel or probe tack test.

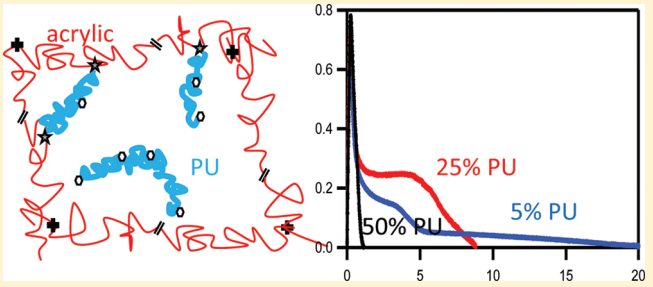

INTRODUCTION

Pressure-sensitive adhesives (PSA) are soft polymeric materials displaying an instantaneous adhesion on most surfaces upon application of a light pressure. Although the function appears relatively simple, the design of proper PSA is complex and relies heavily on polymer chemistry (for acrylic and silicone polymers) or on formulation (for block copolymers and natural rubbers) in order to obtain sparsely cross-linked polymer networks with optimized properties.[2−7] This optimization means that the PSA must be able to dissipate energy during the peeling process (a property optimized for a highly viscous entangled polymeric liquid) and must be resistant to creep in shear (optimum when some cross-linking is present preventing flow).

Acrylic PSA[4,8] are generally weakly cross-linked copolymers of low T_g which have insoluble and soluble fractions, called gel and sol, respectively. A very broad molar mass distribution (i.e., high polydispersity) of the sol fraction and a cohesive network formed by the gel is a good and relatively easy way to achieve a practical solution but has limitations due to the impossibility of independently control the architecture of sol and gel during a simple synthesis. The fine control of the network structure of the gel becomes an essential aspect of advanced techniques to achieve a better balance of properties.

A possible design path to achieve a better control of the network structure is to incorporate another polymer (such as an alkyd or a polyurethane) to form hybrid materials. The preparation of these hybrid materials could potentially lead to a more favorable combination of properties compared with those of the initial purely acrylic PSA. Because of environmental concerns, however, we have focused our study on emulsion-based acrylic PSA.[8] In emulsion-based systems, the independent control of the network structure of the gel and of the sol fraction is more difficult. Furthermore, the control of the interfaces between particles remaining after drying is problematic and can strongly affect the mechanical properties.[9,10]

The development of miniemulsion polymerization[11,12] has helped to overcome the main issue of the homogeneous incorporation of a hydrophobic polymer in a waterborne acrylic polymer. The advantage of miniemulsion polymerization is that it is

Received: January 12, 2011
Revised: March 4, 2011
Published: April 04, 2011

possible to directly incorporate a hydrophobic polymer (e.g., PU) into the monomer droplets and then directly polymerize the droplets to get a hybrid where the components are mixed at the nanometer scale.[12] If these hydrophobic compounds contain reactive functional groups, such as unsaturated double bonds, then they can be chemically incorporated into the growing polymer chains during the free radical polymerization.

Many different components have been incorporated successfully into hybrid systems in this manner, and several reviews are available presenting the technique and the possibilities of hybridization.[11−14]

A number of studies have investigated the synthesis of acrylic−polyurethane (PU) systems. Successful incorporations have been reported by the formation of interpenetrating networks,[15] by the formation of a core−shell structure,[16] or by standard emulsion polymerization with a polyurethane dispersion as a seed.[17] In all cases, the transparency and homogeneity of the hybrid were better than those of the physical blends. However, miniemulsion polymerization appears to be a versatile and powerful method to graft polyurethane to an acrylic polymer as exposed in the work of Udagama et al.,[1] of Wang et al.,[18−22] or again of Li, El-Aasser, and co-workers.[23] In the latter study, it is shown that the grafting prevents phase separation at the particle scale between polyurethane and acrylic copolymer. Most studies focused on applications as coatings, where advantages of combining acrylic with urethane for PSA applications are potentially numerous: better film formation, better mechanical stability or temperature resistance,[23−25] and where a precise control of the polymer architecture is not necessary since cross-linkers (dryers) are often added. To the best of our knowledge, ours is the first study focusing on acrylic polymers for adhesive applications where the control of the polymer architecture is essential to obtain the desired properties and where a precise control of a low level of cross-linking[26] and of the entanglement structure is essential.[27]

In this study and in its companion paper,[1] we selected a model acrylic copolymer typical of those used for PSA and investigated the incorporation of a minority fraction of a low molar mass reactive PU in the acrylic particle. Part I[1] focuses on the synthesis methods while part II, the current paper, focuses on the effect of changing synthesis parameters on the adhesive properties and relates such changes to the network structure, characterized by mechanical tests on dry films and by swelling experiments.

EXPERIMENTAL SECTION

Synthesis. All samples have been synthesized in batch via miniemulsion polymerization. The details of the polymerization procedure are described in a companion paper,[1] and we only briefly recall here the main synthesis parameters which are necessary to understand the results.

The monomer composition of the acrylic matrix was butyl acrylate (BA, 89.5 wt %), methyl methacrylate (MMA, 9.5 wt %), and acrylic acid (AA, 1 wt %). A NCO-terminated polyurethane (PU) prepolymer (Incorez 701, Industrial Copolymers Limited) was incorporated in the acrylic polymer particles. This incorporation was performed in three steps:

(1) The PU prepolymer chains were dissolved in the organic monomer phase, which also contained the hydrophobic costabilizer: octadecyl acrylate (ODA). Hydroxyethyl methacrylate (HEMA) was added, and a known amount of NCO functions was reacted with a known amount of HEMA. We thus define the percentage of HEMA to NCO (% HEMA to NCO). This step was conducted for 12 h at 25 °C using dibutyltin dilaurate as catalyst and results in the grafting of NCO to the HEMA.

Table 1. Description of the Different Series of Latexes

lab code	CTA[a]	PU[a]	HEMA (mol % to NCO)	OH/NCO	HEMA/BPA[b]
T150	0.2	5	10	0.55	0.22
T151	0.2	15	10	0.55	0.22
T152	0.2	35	10	0.55	0.22
T153	0.2	50	10	0.55	0.22
T147	0.2	25	5	0.55	0.11
T145	0.2	25	10	0.55	0.22
T148	0.2	25	15	0.55	0.36
T149	0.2	25	20	0.55	0.50
T160	0.3	25	10	1	0.10
T161	0.2	25	20	1	0.25
T170	0.2	0			

[a] Wt % relative to monomers. [b] Molar ratio of the OH groups from HEMA to the OH group from BPA.

(2) A known amount of Bisphenol A (BPA) was added to the organic phase containing PU and the dibutyltin dilaurate catalyst and reacted for 30 min at 25 °C. The role of this BPA was to extend the PU chains and complete the reaction with the remaining NCO groups.

(3) The organic phase containing the monomers and the HEMA-functionalized BPA-extended PU chains were added to the aqueous solution containing surfactant (Dowfax 2AI). Nanodroplets were formed by ultrasonication. The radical polymerization was initiated with the addition of a redox initiator pair (*tert*-butyl hydroperoxide, TBHP, and sodium formaldehyde sulfoxylate, SFS), and miniemulsion polymerization was carried out at 50 °C.

1-Dodecyl mercaptan was used as a chain transfer agent (CTA) to control the kinetic chain length and therefore gel formation. 0.2 wt % with respect to monomers was added unless mentioned otherwise. Three series of samples were prepared varying sytematically the molar ratio between OH and NCO functions, the molar ratio of OH functions from the HEMA to OH functions from the BPA (the HEMA/BPA ratio), and the polyurethane weight fraction. Table 1 summarizes the important formulation parameters for the different samples.

Polymer Characterization. The solid content of the latexes was measured gravimetrically and was ∼50 wt % of polymer for all latexes.

We measured the gel content and the swelling ratio, Q, by static measurements. A small piece of solid film was cut and weighed (W_1) and was then immersed in THF for a week. After a week, the sample was taken out and weighed again (W_2). It was then dried at 60 °C for 30 min to extract all the solvent, and the dried sample was weighed (W_3).

The gel content was given by

$$\%\ \text{gel} = \frac{W_3}{W_1} \times 100 \tag{1}$$

and the swelling ratio by

$$Q = \frac{W_2}{W_3} \tag{2}$$

The glass transition temperature of the final polymer samples (T_g) was measured by differential scanning calorimetry (DSC; TA Instruments DSC 2920). Two cycles were performed at cooling and heating rates of 10 °C min^{-1}. The T_g was obtained from the second cycle.

Mechanical Characterization. Samples for the rheological and tensile experiments were prepared as follows: a given volume of latex was deposited in silicone molds and dried at room temperature for 1 week. The molds were covered with a bell jar to protect them from dust. The volume of latex was calculated to give the required final film thickness

depending on the latex solid content. After a week, the molds were held for 5 min at 110 °C. The samples were then removed, placed between low-release silicone papers, and cut to the desired dimensions with a die cutter.

For the probe tack experiments, the latexes were deposited on microscope glass slides also protected from dust by a bell jar and dried 48 h at room temperature. They were finally dried for 1 min at 110 °C, and the resulting films, with an average thickness of 120 μm, were kept in plastic boxes before use. All samples were used within a week of preparation.

The linear viscoelastic properties of the adhesives were characterized with a rheometer RDAII using parallel plate geometry. Frequency sweeps (0.3−120 rad s^{-1}) with an applied strain between 5% and 10% were made on 500 μm thick samples of 8 mm as diameter at room temperature.

For the large-strain behavior, we used a standard tensile INSTRON machine (model 5565) equipped with a video extensometer (model SVE) and a 10 N load cell with a resolution of ±1 mN. Rectangular strips of 5 mm wide (w_0) with an average thickness (e_0) of the order of 500 μm were cut within the self-standing films. Individual values were controlled for each sample. The initial velocity of the crosshead was chosen to obtain an initial strain rate of 1 s^{-1}, which is roughly equivalent to the initial strain rate applied during the adhesion tests, and all tests were performed at room temperature. The force−displacement curves obtained were then converted to nominal stress $\sigma_N = F/A_0$ vs stretch $\lambda = l/l_0$.

The adhesive properties were characterized with two types of tests: a laboratory probe test[28,29] and a series of standard industrial tests. In the probe tack test, a stainless steel probe comes in contact with the adhesive layer deposited on a glass slide. After a set contact time, the probe is withdrawn at a constant velocity. A mirror is installed upon the glass slide and allows the visualization of the debonding mechanism and the measurement of the real contact area for each sample. We used standard parameters for the temperature (room temperature), approach velocity (V_{app} = 30 μm s^{-1}), contact time (t_c = 1 s), and contact force (F_c = −70 N). The debonding rate was varied between 1 and 1000 μm/s, but we report here only data for the debonding velocity (V_{deb} = 100 μm s^{-1}) for the purpose of comparing materials. The force was measured by a load cell (250 N, resolution 0.5 N). The displacement of the probe was measured with an LVDT extensometer (range 5 mm, resolution 0.5 μm). The force and displacement for each curve were normalized by the contact area of the probe (as visualized with the camera) and by the initial thickness of the film to obtain a stress vs strain curve, which will be used to compare adhesive films. The adhesion energy W_{adh} was defined as the integral under the stress vs strain curve multiplied by the initial thickness of the film.

The characterization of the adhesive properties of the films with industrial standard tests (FINAT) was carried out as follows. The latexes were dried on a polyester (PE) backing film for 3 min at 110 °C to obtain dry adhesive film thicknesses of 23 μm which are standard in industry. These adhesive + PE layers were then bonded to a stainless steel (SS) substrate.

The shear resistance was defined by measuring the holding time (in minutes) before failure of a 1 $in.^2$ adhesive layer, to which a mass of 1 kg was applied (FINAT test method 8). The maximum time measured was 10 000 min. After this limiting time, the test was stopped. If a cohesive failure occurred, CF was noted along with the value of the holding time at failure. It is worth noting that for a commercial PSA cohesive failure is neither desirable in the case of the shear resistance test nor in the case of the probe test.

RESULTS AND DISCUSSION

Before discussing the specific effects of the PU weight fraction and of the degree of grafting, it is useful to briefly summarize the DSC results. The PU has no apparent effect on the heat capacity scans, and a single T_g of −39 ± 3 °C is detected for all hybrid adhesive films. For comparison, the T_g of the pure PU is estimated to be around −48 °C. Therefore, the large distribution of the T_g of the copolymer and its proximity with the T_g of the PU could mask a possible phase separation.

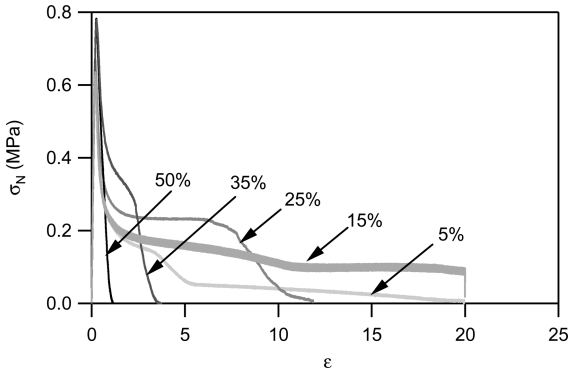

Figure 1. Stress−strain tack curves for the different PU weight fractions with 0.2% CTA and HEMA/BPA = 0.22; V_{deb} = 100 μm s^{-1} (i.e., dε/dt = 1 s^{-1}).

Role of the PU Weight Fraction. *Adhesive Properties.* In the first series of samples (samples T150 to T153 in Table 1), the effect of the weight fraction of reactive PU incorporated in the polymer was investigated. Figure 1 presents probe tack results for this series. The relevant parameters chosen to analyze these results were the plateau stress at intermediate and larger strain and the maximum strain. The plateau stress σ_f is related to fibrillation observed during the debonding, while the maximum strain ε_{max} corresponds to the final detachment from the probe.[28] Figure 1 shows that samples with a low amount of polyurethane (less than 25% based on the total amount of acrylic monomers) are characterized by a low fibrillation stress and a high maximum strain ε_{max}.[50] The residues remaining on the probe after the test indicate a cohesive debonding inside the fibrils. These tack curves are characteristic of samples with a low level of elasticity due to a low level of cross-linking. On the other hand, for samples with 35 or 50 wt % of PU, the tack curves show almost no fibrillation plateau and the ε_{max} is low. Despite nucleation of cavities at the onset of debonding, these cavities coalesce and interfacial propagation of cracks leads to an interfacial debonding.[30,31] Finally, the sample with 25% of PU forms a fibrillar structure upon debonding and debonds at a maximum strain ε_{max} of the order of 10, which is typical of many commercial PSA's. The final drop of the stress is characteristic of adhesive debonding and results in the absence of residues on the probe. Thus, adhesive properties are best for this fraction of PU.

Table 2 presents results from probe tack tests, gel measurements, and industrial shear tests. The comparison between probe test results, which measure the energy dissipated during fast debonding and shear resistance, which is a measure of the resistance to failure at long times, shows similar trends. The best compromise in properties appears to be the sample with 25% PU which combines an improvement in tack and a 50-fold increase in shear resistance. The most interesting result here is the comparison of the best hybrid PSA (T145) with the pure acrylic matrix (T170), showing that both adhesion energy and resistance to shear have been improved by the incorporation of the PU in the material.

Table 2. Adhesion Energy Measured for V_{deb} = 100 μm s^{-1} and Industrial Shear Resistance Results

sample name	PU (wt %)	gel fraction (%)	W_{adh} (J m^{-2})[a]	shear resistance (min)
T170	0	47.3	200.4 ± 21.2	181 ± 15 CF
T150	5	not measurable	161.4 ± 43.2 CF	46 ± 15 CF
T151	15	25.7	379.3 ± 111.3 CF	222 ± 15 CF
T145	25	37.4	284.9 ± 93.3	9463 ± 15 CF
T152	35	57.9	143.62 ± 39.9	not measured
T153	50	73.8	49.6 ± 5.2	>10 000

[a] For V_{deb} = 100 μm s^{-1}.

The interpretation of these results requires a finer characterization of the differences in the network structure.

This characterization was carried out with the help of three different methods which are complementary: Rheological measurements reveal the level of viscoelasticity, large strain tensile experiments are a sensitive probe of the finite extensibility of the network chains and of the dissipation of energy taking place at large strains, and the swelling and gel fraction measurements inform on the architecture of the polymer.

Linear Viscoelasticity. Since decades the linear viscoelastic properties of pressure-sensitive adhesives have been considered the best predictor of the adhesive properties.[32−35] From fully empirical criteria, we have now moved to more mechanistically based semiempirical criteria which are able to predict to a certain extent the performance of PSA.[30]

Figure 2 shows the variation of the storage modulus and tan δ with frequency, for three adhesive films with increasing PU content. At equivalent degree of grafting, the more PU is added to the hybrid, the higher is its elastic modulus and the lower is tan δ. This shows that the number of pendant chains and free chains decreases significantly with PU content. It also suggests that the entanglement density (at high frequency at room temperature) increases with PU content.

Following the methodology proposed by Deplace et al.,[30] these linear viscoelastic properties, and in particular the value of tan δ/G' at the relevant debonding frequency, can be used to predict the suitability of the soft network for PSA applications.

The value of 25 wt % of PU in the latex represents an optimum value for the viscoelastic properties as well. Indeed, both the stiffness and the fibrillation (tan δ/G') criteria are fulfilled with G'(1 Hz) equal to 99 000 Pa (below the Dahlquist criterion[36]) and tan δ/G' equal to 0.6 × 10^{-5} Pa^{-1} at 1 Hz, and fibrillation debonding is indeed observed.

The differences in viscoelastic behavior reflect differences in the architecture of the polymer inside the particle. Table 2 gives the gel fraction in the adhesive film for the five PU contents. For 5% PU, the gel fraction is too low to be measured. Then it increases to 70−80% for the high PU content samples.

The characterization of the gel fraction is a good indicator of the viscoelastic behavior. The partially cross-linked gel imparts elasticity while the pendant chains attached to the gel and the sol fraction control the time-dependent stress relaxation. On the basis of the differences in linear viscoelastic properties and gel fraction, the incorporation of PU at fixed grafting ratio increases the cross-link density and the entanglement density (high frequency G'), and decreases the density of pendant chains and the soluble fraction.

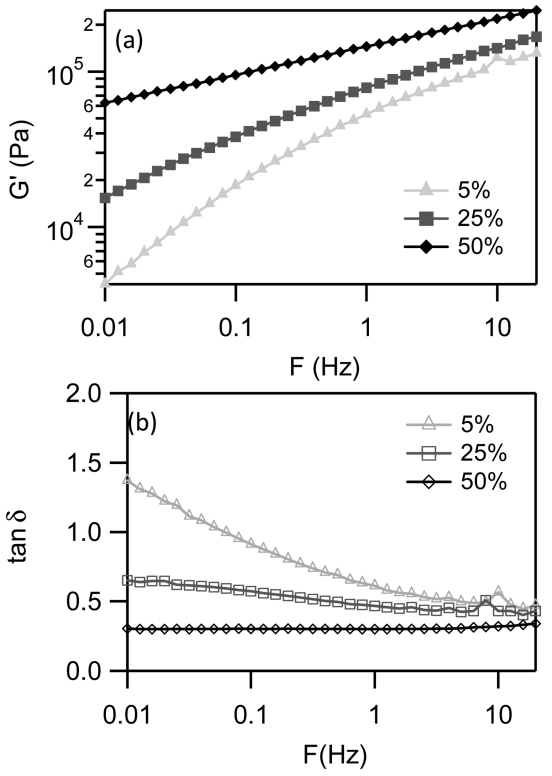

Figure 2. Evolution of G' (a) and tan δ (b) as a function of frequency for different PU weight fractions: 5 wt % (T150), 25 wt % (T145), and 50 wt % (T153). T = 25 °C.

Large Strain Behavior. While linear rheology experiments are useful to predict whether fibrils will form or not after the initial cavitation stage, the final detachment of these fibrils can only be predicted through the analysis of the large strain behavior.[37−39] Figure 3 shows the results of tensile experiments for the five samples with different amounts of PU. Very significant differences due to the presence of PU are immediately apparent not only in the absolute values of the stress at equivalent strain but also in the overall shape of the stress−strain curve. The two samples with the lowest PU weight fractions (T150 and T151) do not present any hardening at large strain but simply flow at a nearly constant nominal stress.

The tensile behavior of these weakly cross-linked networks is highly nonlinear and shows a pronounced relaxation or softening after about λ = 1.5. For almost all PSA's this softening is both strain and strain rate dependent, and curves measured at a single strain rate can be fitted equally well by a viscoelastic model[26] or by a nonlinear elastic model.[40] However, if tensile tests are carried out at two different strain rates with the same material, it is impossible to fit both curves with the same material parameters with either model. A quantitative modeling of the large strain behavior of a PSA would require a full fledged nonlinear viscoelastic model including finite extensibility. Such a model has not yet been developed. However, it is possible to use a simpler and approximate methodology to characterize the PSA behavior in large strain.

First, the Young's modulus E_y can be measured at small strains. It is defined as the slope of a line fitting the curve between λ = 1 and λ = 1.02. This quantity represents the unrelaxed modulus and should be directly comparable with $G'(\omega)$ at the appropriate strain rate.

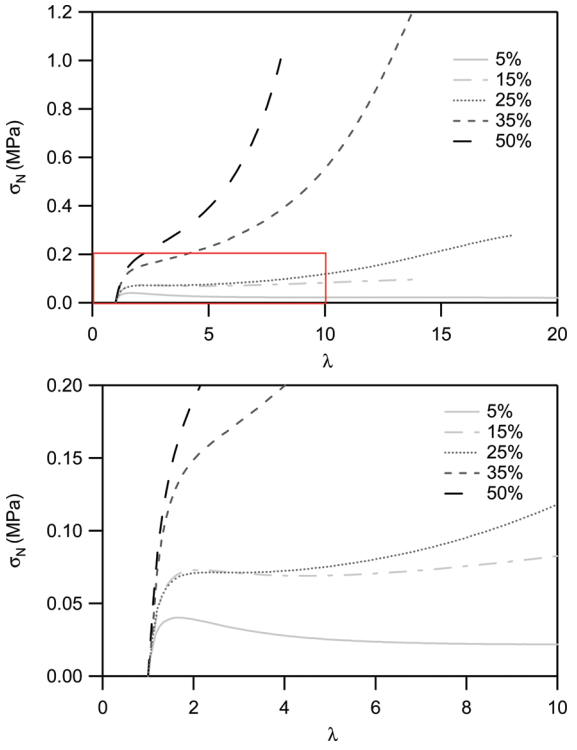

Figure 3. Nominal stress versus λ for the five different PU weight fractions; $d\varepsilon/dt = 1\ s^{-1}$. The bottom figure is a magnification of the red square.

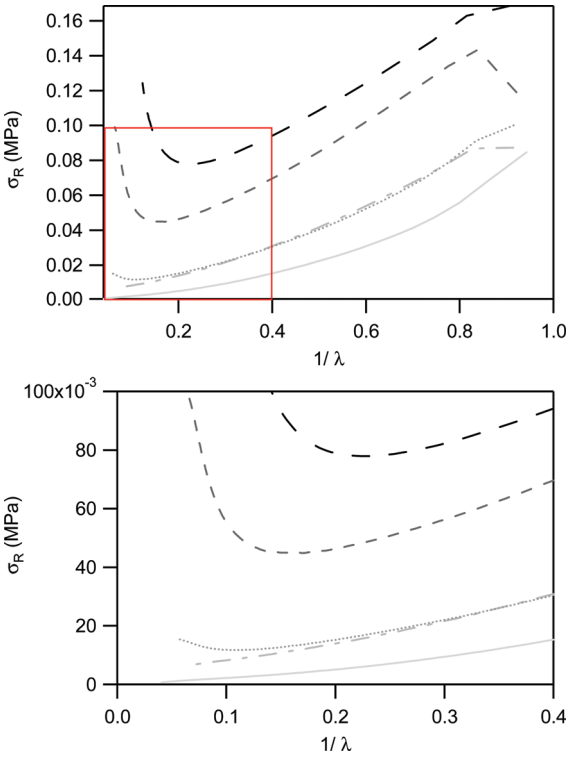

Figure 4. Reduced stress versus $1/\lambda$ for the five different PU weight fractions; $d\varepsilon/dt = 1\ s^{-1}$. The bottom figure is a magnification of the region in the red square.

Second, the deviation of the stress−strain curve relative to the prediction from Gaussian rubber elasticity can be analyzed from the Mooney representation. The reduced stress σ_R, also named Mooney stress, is defined as

$$\sigma_R = \frac{\sigma_N}{\lambda - \frac{1}{\lambda^2}}$$

It corresponds to the nominal stress normalized by $\lambda - 1/\lambda^2$. For a neo-Hookean rubber, the reduced stress is constant as a function of λ and is simply equal to the shear modulus G. For a PSA, this reduced stress is not constant and is typically represented as a function of the inverse of strain $1/\lambda$.[30] Two characteristic parameters of the nonlinear behavior can be determined: the C_{soft} to characterize the softening at intermediate strain and the C_{hard} characterizing the onset of strain hardening at large strain.[30] C_{soft} is defined as the slope of a line drawn between $(\sigma_R(0.8);\ 1/\lambda = 0.8)$ and $(\sigma_{Rmin};\ 1/\lambda_{min})$. C_{hard} is defined as the reduced stress corresponding to the minimum in σ_R. Another interesting parameter is λ_{hard}, i.e., the strain level corresponding to the minimum reduced stress and hence to the onset of strain hardening. The physical meaning of C_{soft}, C_{hard}, and λ_{hard} can be inferred from molecular models of elasticity of rubber networks such as that proposed by Rubisntein and Panyukov,[41] which combines entanglements and cross-links, or that proposed by Edwards and Vilgis[42] combining entanglements, cross-links, and finite extensibility. C_{soft} represents the density of entanglements while C_{hard} represents the density of cross-links. λ_{hard} is, on the other hand, related to the finite extensibility of the chains.

Table 3. Values of the Mooney−Rivlin Viscoelastic Parameters for Different PU Amounts; $d\varepsilon/dt = 1\ s^{-1}$

sample code	PU (wt %)	C_{soft} (kPa)	C_{hard} (kPa)	C_{soft}/C_{hard}	E (kPa)
T150	5	84.5	no min in σ_R	∞	141.4
T151	15	115.9	no min in σ_R	∞	239.7
T145	25	109.4	11.8	9.3	275.6
T152	35	147.3	44.8	3.2	329.6
T153	50	143.6	77.9	1.8	459.9

The Mooney representations as a function of PU content are shown in Figure 4 while Table 3 gives the values of the viscoelastic parameters C_{soft} and C_{hard}, the ratio C_{soft}/C_{hard}, and the Young's modulus.

The ratio C_{soft}/C_{hard} reflects the balance between the extent of relaxation at intermediate strain and hardening at large strain. It decreases significantly with increasing PU content, reflecting the less and less viscoelastic character of the films (see Table 3). The Young's modulus is a small-strain high-frequency modulus, affected by both chemical cross-links and entanglements (which are all trapped at high frequencies). However, in a fully acrylic matrix it is usually not much affected by a low level of cross-linking.[26,40] Its increase with PU content indicates that the network has clearly more entanglements with increasing PU. The increase of C_{hard}, on the other hand, only reflects the increase in chemical cross-links. The nonmeasurable density of such cross-links for 5 and 15 wt % of PU is fully consistent with the observed cohesive failure of these two adhesives in the tack experiments. The absence of strain stiffening at large strains prevents the fibrils from detaching from the surface without leaving residues.

dx.doi.org/10.1021/ma2000702 |*Macromolecules* 2011, 44, 2643–2652

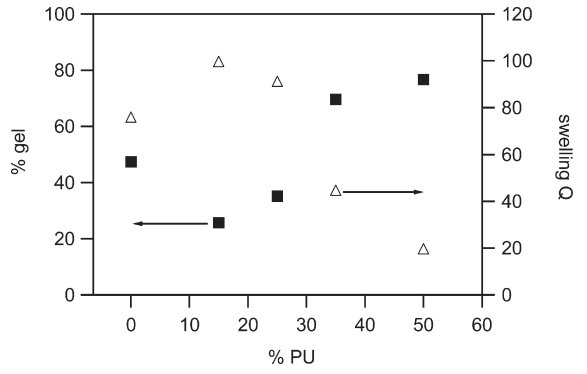

Figure 5. Evolution of the gel fraction (■) and of the swelling ratio (△) with the polyurethane content.

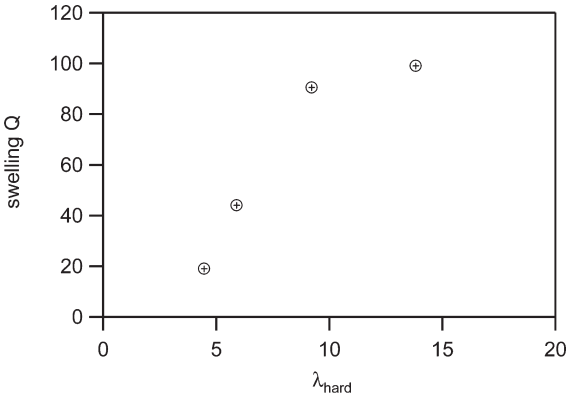

Figure 6. Evolution of the swelling Q with the hardening strain λ_{hard}.

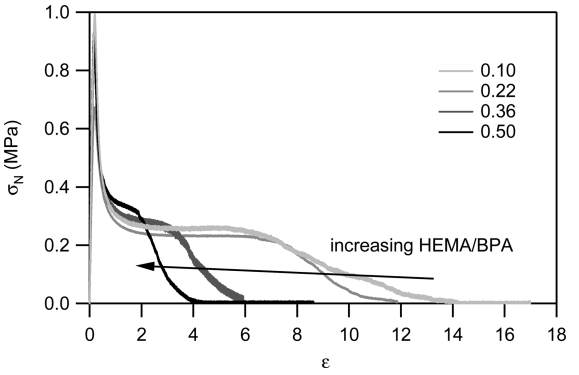

Figure 7. Stress−strain tack curves for four different HEMA/BPA ratios; V_{deb} = 100 μm s^{-1} (i.e., dε/dt =1 s^{-1}).

Figure 5 shows the change in gel fraction and equilibrium swelling of the gel as a function of PU content. The sharp increase in gel fraction with PU content is consistent with the viscoelastic measurements: If the equilibrium swelling is compared in Figure 6 with the hardening strain λ_{hard} obtained from tensile experiments of the films, λ_{hard} decreases with the equilibrium swelling Q, which indicates that the PU chains considerably shorten the average length of the acrylic chains between cross-link points. This is due to the fact that, at fixed stoichiometry, more PU means more HEMA and hence more grafting points. Therefore, the average molecular weight between grafting points on the acrylic chains decreases.

Discussion. These combined results indicate that the network becomes much more densely cross-linked when the PU weight fraction increases. However, it is interesting to note that a small amount of PU actually reduces the gel fraction and the strain stiffening, relative to a purely acrylic matrix. This reduction in cross-linking is probably due to a reduction in the acrylic kinetic chain length since the bisphenol A favors chain transfer.[43,44]

The gel fraction and swelling experiments confirm that the NCO-terminated PU enhances cross-linking of the PU polymer chains to the acrylic network through the HEMA. In essence, the PU would appear to act like any low molecular weight cross-linker.

Yet this is misleading because, in addition, PU chains are also more densely entangled than the acrylic chains because of the PPG constituting their soft segment ($M_e \sim 3-5$ kg mol^{-1} for the PU[45] while $M_e \sim 20-30$ kg mol^{-1} for the acrylics[46,47]). Thus, the PU adds both chemical and physical cross-links, and this is the reason for the significant increase in the small-strain modulus. The very significant softening observed for all PU hybrids would be very difficult to obtain with a purely acrylic network.

The consequence on adhesive properties of this continuous variation in cross-linking and entanglement density with PU content is a clear transition from under-cross-linked to over-cross-linked materials. Only one of the adhesives gives a network architecture adapted to a PSA application and a reasonable balance between relaxation and hardening. This sample debonds adhesively in a fibrillation mode, with relatively high adhesion energy. An equivalent optimum in the PU weight fraction has been observed by Wang et al.[20] in the same type of PU/acrylic hybrid prepared for coating applications.

Impact of the Degree of Grafting of the PU. If the PU content is fixed, the second parameter that can be varied is the level of grafting of the PU chains to the acrylic matrix. The reaction between HEMA and NCO-terminated PU can be well controlled during the synthesis.[1] In the following series, the fraction of NCO actually consumed during HEMA grafting is varied from 5 to 20 mol %, taking into account that 20% is the maximum level of grafting allowed by the reaction between HEMA and PU.[1] For a fixed total amount of OH groups, the degree of grafting is directly connected to the HEMA/BPA molar ratio. In this section, we compare samples with a constant weight fraction of PU (25%) and HEMA/BPA ratios changing from 0.1 to 0.5 with a ratio between OH and NCO fixed at 0.55.

Adhesive Properties. Figure 7 shows the probe tack curves obtained for different degrees of grafting at a PU content of 25% and a CTA amount of 0.2%. For these synthesis conditions, a fibrillation plateau is always observed, but cohesive failure of fibrils is sometimes observed for the sample with HEMA/BPA = 0.10. The maximum deformation ε_{max} of the adhesive layer decreases markedly when the ratio HEMA/BPA increases and the fibrillation stress σ_f of the tack curves increases with HEMA/BPA.

As shown in Table 4, the low grafting regime is particularly interesting. While increasing the adhesion energy relative to the pure acrylic matrix, the resistance to shear increases dramatically.

Linear Viscoelastic Properties. G' and tan δ as a function of frequency for different HEMA/BPA ratios with 25 wt % of PU are shown in Figure 8. The resulting values of tan δ/G' are all predicting a fibrillation debonding, and the grafting ratio at fixed PU content does not greatly affect the linear viscoelastic properties.

Table 4. Adhesion Energy Measured at V_{deb} = 100 μm s^{-1} and Industrial Shear and Peel Results for the Blank Sample and the Four HEMA/BPA Ratios (In All Cases OH/NCO = 0.55)

sample name	HEMA/BPA	W_{adh} (J.m^{-2})	shear resistance (min)
T170	0.0	200.4 ± 21.2	181 ± 15 CF
T147	0.11	548.4 ± 128.2	1680 ± 15 CF
T145	0.22	284.9 ± 93.3	9463 ± 15 CF
T148	0.36	164.6 ± 21.3	>10000

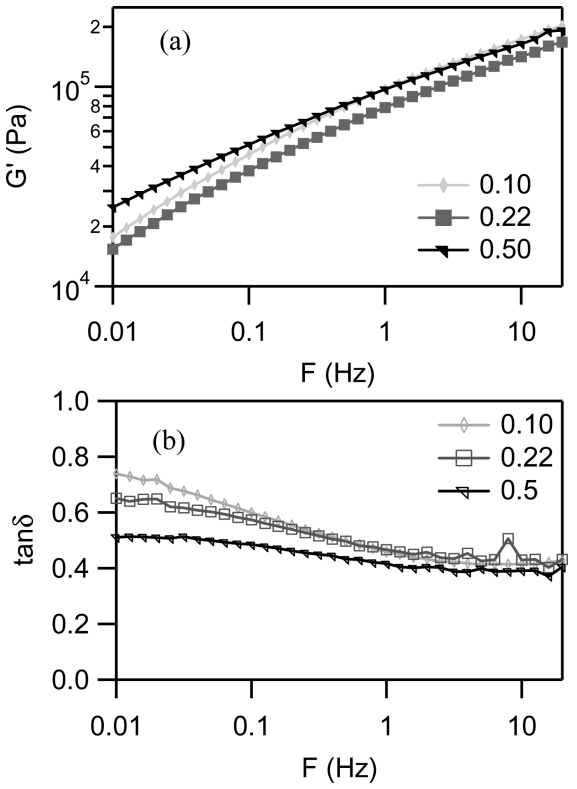

Figure 8. Evolution of the G' (a) and of the ratio tan δ/G' (b) as a function of frequency for HEMA/BPA = 0.10 (T147), for HEMA/BPA = 0.22 (T145), and for HEMA/BPA = 0.50 (T149); $\varepsilon \sim 8\%$.

This relative insensitivity of the linear viscoelastic properties with grafting ratio are confirmed by the gel fraction measurements which all show a gel fraction varying between 36 and 54% and increasing slightly with increasing HEMA/BPA ratio.

Large Strain Experiments. The tensile experiments are more sensitive to the subtle changes in polymer architecture, and they have been performed on the same samples at a nominal strain rate $d\varepsilon/dt = 1\ s^{-1}$. To emphasize these fine changes, we choose here the Mooney representation, as explained in the Large Strain Behavior subsection (Figure 9). The different curves have a similar shape for all the HEMA/BPA ratios. The main difference is in the onset of strain hardening. The increase of C_{hard} shows that HEMA/BPA mostly affects the density of permanent cross-links, i.e., the bridges created by the PU chains, but not the finite extensibility of the network presumably controlled by the longer chains of the acrylic network. Such an apparently conflicting result can only be obtained with a heterogeneously cross-linked network, i.e., some densely cross-linked zones (which swell less

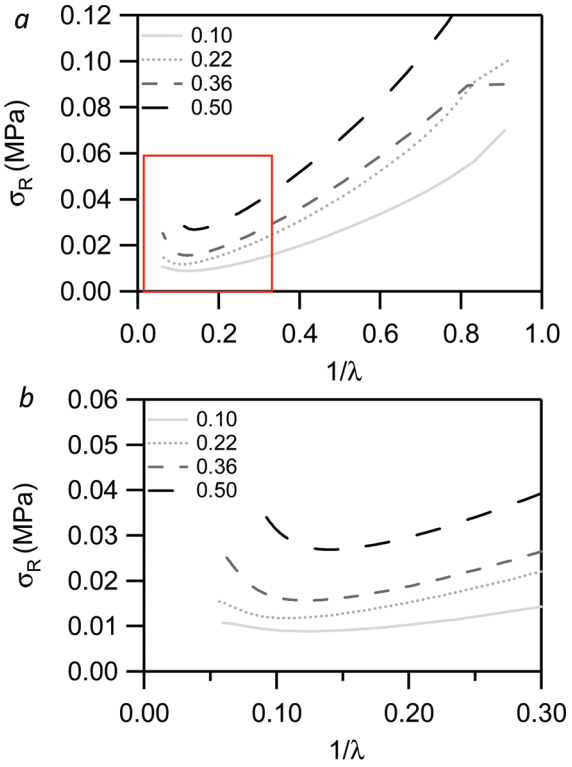

Figure 9. (a) Reduced stress versus $1/\lambda$ for the different HEMA/BPA ratios; $d\varepsilon/dt = 1\ s^{-1}$. (b) Magnification of the area within the red square in (a).

Table 5. Values of the Mooney−Rivlin Viscoelastic Parameters for the Four Different HEMA/BPA Ratios; $d\varepsilon/dt = 1\ s^{-1}$

sample name	HEMA/BPA	C_{soft} (kPa)	C_{hard} (kPa)	C_{soft}/C_{hard}	E_y (kPa)
T147	0.11	67.9	8.9	7.7	191.5
T145	0.22	109.4	11.8	9.3	275.6
T148	0.36	106.5	15.65	6.8	244.7
T149	0.50	116.2	26.9	4.3	414.9

and provide stiffness) and some less cross-linked zones which percolate and can extend. The values of C_{soft} (Table 5) remain relatively constant except for the lowest grafting density where the relaxation is very fast, and as a consequence the value of C_{soft}/C_{hard} decreases with grafting density.

Measurements of the gel fraction and small strain modulus confirm this scenario.

Discussion. The cross-linked network architecture is modified by the HEMA/BPA ratio but differently than by the PU content. Decreasing the HEMA/BPA ratio is equivalent to decreasing the density of PU bridges incorporated in the network. However, this time this change occurs mostly in the gel fraction and does not greatly affect the finite extensibility of the network probably because of a heterogeneous gel structure. As a result, the adhesion energy remains relatively constant, but the material can be made a little less cross-linked (favorable for adhesion on low-energy surfaces) or more cross-linked (favorable for high shear resistance).

One can conclude that at fixed 25% PU content the change in grafting ratio affects the cross-linking density of more cross-linked

dx.doi.org/10.1021/ma2000702 |*Macromolecules* 2011, 44, 2643–2652

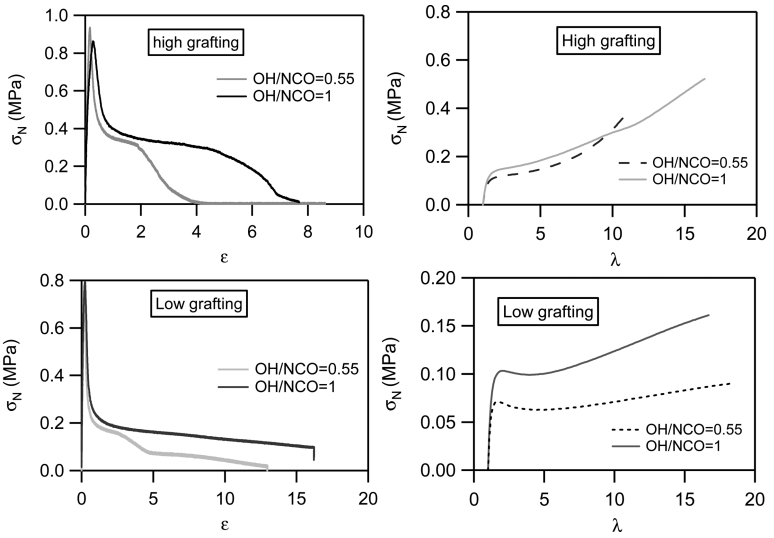

Figure 10. Probe tack (left) and tensile results (right) of samples with OH/NCO = 0.55 and OH/NCO = 1 for high grafting of PU (top; samples T149 and T161) and low one (down; samples T147 and T160); for probe tack tests V_{deb} = 100 μm s^{-1} (i.e., dε/dt = 1 s^{-1}); for tensile tests dε/dt = 1 s^{-1}.

domains in a heterogeneous gel structure and does not affect much the sol fraction. It affects the low-frequency dissipation in the polymer network, improving the resistance to flow, and not the small strain and high-frequency elasticity. It is then possible to use separate synthetic tools to adjust the storage modulus (PU fraction) and the finite extensibility (PU grafting).

Effect of the OH/NCO Ratio. As described in a companion paper, during the miniemulsion synthesis, it is necessary to add a hydrophobic monomer to avoid Ostwald ripening of particles.[12] Here 5.15% in weight (relative to the monomer content) of octadecyl acrylate (ODA) was incorporated in the recipe. In the presence of this hydrophobic component, it was not possible to incorporate the total amount of BPA required to give a stoichiometric ratio OH/NCO = 1. For amounts higher than 50% of the theoretical amount, flocculation of the particles was observed during the synthesis.[1]

The consequence for the polymer architecture and mechanical properties is that the PU chains are expected to be less extended by BPA. Furthermore, as no isocyanate can be observed by ^{13}C NMR, it is reasonable to assume that reaction with water occurs. In other words, the reaction of polyurethane prepolymer chains is not completely controlled.

To promote a total reaction of the remaining isocyanate with BPA, some samples have been prepared without costabilizer ODA and with OH/NCO = 1. No flocculation was observed and films have been prepared from these new latexes. In these samples, 25 wt % of PU is incorporated, and two grafting ratios of the PU were chosen: 20% (high grafting) and 10% (low grafting). CTA content also varied from 0.2% for the high grafting to 0.3% for the low grafting (see Table 1). Probe tack and tensile results of four samples are presented in Figure 10.

The effect of the change in process is different in the case of high grafting level and low grafting level (Figure 10). Nevertheless, in both cases, the increase in the amount of BPA has a positive effect.

For high grafting the deformability of the sample is significantly improved. The polymer network is more deformable with equivalent small-strain stiffness. Our hypothesis is that the presence of BPA may act there as a chain transfer and reduce the kinetic chain length of the acrylic, effectively making the hybrid network a bit more viscoelastic and extensible. This confirms the hypothesis of longer acrylic chains formed with the presence of a higher amount of BPA and thus higher deformability. The gel and swelling measurements partially confirm this interpretation. The gel content decreases from 54.5% for OH/NCO = 0.55 (less BPA) to 44.3% for OH/NCO = 1 (more BPA), and the swelling increases from 57.0 (less BPA) to 74.6 (more BPA). They indicate that the network is less cross-linked, but with only a small effect of the decrease in the gel fraction on the elasticity.

For low grafting, probe tack tests show a longer plateau, due to a stabilized fibrillation process. In tensile experiments the softening takes place at a higher stress, and hardening is more pronounced. These observations reflect that the material is less deformable with more BPA. In this case, it may be argued that the extension of PU chains by BPA can help to connect dangling chains together to create PU bridges and increase the gel content and thus the stiffness. Unfortunately, the extraction and swelling measurements could not be done due to the low level of cross-linking in the samples.

If the effect of the extension on the mechanical properties (see Figure 11) is clear in both cases, it is not easy to locate the transition from the first mechanism (reduction of acrylic chain length) to the second one (formation of new PU bridges), and the effect of reaction with water is also unclear.

On the point of view of the application as PSA, the best results in tack, peel, and shear are obtained for hybrid latexes with 25% of polyurethane compared to the acrylic monomers, with OH/NCO = 1, HEMA/BPA ~ 0.25, and 0.2% CTA.

General Discussion: Network Structure of the Urethane/Acrylic Hybrids. Several molecular analysis have demonstrated three ideas.[1] First, all NCO groups have reacted with HEMA, BPA, or water. Then, SEC analysis and inverse titration have shown that the molar mass of the PU prepolymer is ~3000 g mol^{-1}, and finally it is known that only a maximum of 20 mol % of NCO groups can react with HEMA. Therefore, PU chains can be incorporated in three different ways:

BPA-extended chains which have reacted on both side with HEMA form bonded PU chains. After acrylic polymerization, these chains will be part of the gel fraction.

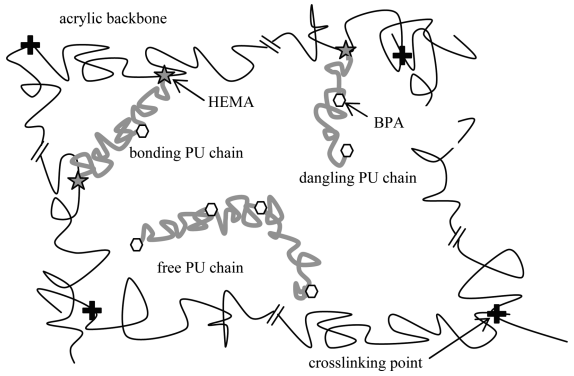

Figure 11. Theoretical urethane/acrylic hybrid network.

BPA-extended chains which have reacted on only one side with HEMA are dangling chains. They are terminated either by a BPA or by an amine (obtained after reaction with water). These chains are connected to the acrylic backbone at only one side.

BPA-extended chains which did not react with any HEMA are called free chains. They are part of the soluble fraction inside the particles.

These three types of chains coexist in the particles, and their proportions and lengths obviously change according to the fraction of PU, the ratio OH/NCO, and the ratio HEMA/BPA.

To have an appropriate representation of the architecture of the hybrid network inside particles, one has to take in account two other important parameters. The molar mass of the acrylic copolymers (300−4000 kg mol^{-1} depending on the samples) is much higher than that of the PU, even extended. Then, assuming that the soft chain is mostly polyether (poly(propylene glycol) PPG), the PU chains are much more entangled than the acrylic ones.

Taking in account the different connections of the PU chains, a schematic representation of the network is presented in Figure 11 (except that no reaction of NCO with water is shown).

The presence of PU affects not only the viscoelastic balance but also the finite extensibility of the adhesive layer by connecting the acrylic backbones. As discussed above, even significantly extended PU grafted chains remain shorter than the acrylic chains. Moreover, most of the chains are bonded chains connected to the acrylic at both ends. In this context the onset of strain stiffening is controlled by the length of the acrylic chains between two grafting points. The change in mechanical properties as a function of grafting density suggest that the PU may not be distributed homogeneously in each particle, with some PU-rich zones connected together by PU-poor zones.

Two important caveats need to be mentioned here. First, no reaction with water is considered in this description. In reality, some of the NCO functions will react with water during the miniemulsification process and the early stages of the synthesis reaction.[1,23,48] This fraction may modify the architecture of the polymer.

Second, in all the discussions above, we have ignored the particle morphology and assumed implicitly a homogeneous incorporation of the PU. This is consistent with the appearance of the films which are clear, transparent, and crack-free at least at a macroscopic level. This is also in good agreement with the unique T_g measured by DSC. Nevertheless, the arguments above plead for the existence of heterogeneous structures and a phase separation occurring at the particle scale for 25 wt % of PU and a degree of grafting of 10% cannot be ruled out. The possible existence of these nanodomains, which are more cross-linked but are embedded in a less cross-linked matrix polymer, seem to have little effect on the dissipation of energy during debonding but to greatly strengthen the resistance to shear of the material. This would also be consistent with a recently published study on nanostructured adhesives.[49]

CONCLUSION

The key findings of our study can be summarized as follows:

The amount of polyurethane (at fixed OH/NCO ratio) affected strongly the ratio between soluble and insoluble parts because of the addition of cross-linking points between the NCO-terminated PU chains and the acrylic chains. Moreover, since the polyurethane is more entangled than the acrylic, it also affected the small strain elastic modulus with the incorporation of many entanglements, which behave like permanent cross-links at high frequency but can relax at low frequency or high temperature.

The degree of grafting at fixed PU content (controlled by the ratio between the grafting agent HEMA and the chain extender BPA) plays an important role in the architecture of the insoluble part. The analysis of the tensile tests strongly suggest a heterogeneous particle structure with a minority of more cross-linked PU rich domains and a majority of less cross-linked and percolating PU-poor domains.

As a result of this heterogeneous structure, industrial standard tests on the adhesive properties of the PSA have shown a clear improvement in shear resistance while the adhesion energy remained acceptable for standard applications. This clearly showed that the detailed structure of the gel part of the PSA is as important as the gel fraction itself, a point which has been often neglected so far.

Clearly, the fine control of the polymer structure inside a particle with a bicomponent system remains very challenging. Several reactions compete kinetically and the final result is likely to depend on the details of the procedure and on the details of the composition such as amount of chain transfer agent used, nature of the initiator, and of course temperature of the reaction. Furthermore, the materials studied here have been produced with a batch process relatively far from the conditions used in industrial applications.

Nevertheless, the general trends discovered should be broadly applicable to the design of hybrid networks containing both polycondensation reactions and free radical polymerization. All previous publications on urethane/acrylic networks focused on high-T_g coatings which have much less propensity to chain transfer reactions and are more sensitive to the details of the interfaces between particles.[19,20,23] To our knowledge this is the first study on the design of such a network in soft adhesives.

AUTHOR INFORMATION

Present Addresses

[#]Laboratoire de Physique de Solides, UMR 8502, Université Paris-Sud, Bâtiment 510, 91405 Orsay, France.

ACKNOWLEDGMENT

The EU Framework 6 Integrated Project NAPOLEON NMP3-CT-2005-01184 is acknowledged for the financial support provided to this project.

REFERENCES

(1) Udagama, R.; Graillat, C.; Degrandi-Contraires, E.; Creton, C.; Bourgeat-Lami, E.; McKenna, T. *Macromolecules* **2011**.

(2) Tobing, S. D.; Klein, A. *J. Appl. Polym. Sci.* **2001**, *79*, 2230–2244.

(3) Tobing, S. D.; Klein, A. *J. Appl. Polym. Sci.* **2001**, *79*, 2558–2564.

(4) Satas, D. Acrylic Adhesives. In *Handbook of Pressure-Sensitive Adhesives*, 2nd ed.; Satas, D., Ed.; Van Nostrand Reinhold: New York, 1989; Vol. 1, pp 396−456.

(5) Sobieski, L. A.; Tangney, T. J. Silicone Pressure Sensitive Adhesives. In *Handbook of Pressure Sensitive Adhesives*, 2nd ed.; Satas, D., Ed.; Van Nostrand Reinhold: New York, 1989; Vol. 1, pp 508−526.

(6) Lindner, A.; Lestriez, B.; Mariot, S.; Creton, C.; Maevis, T.; Luhmann, B.; Brummer, R. *J. Adhes.* **2006**, *82* (3), 267–310.

(7) Creton, C.; Hu, G. J.; Deplace, F.; Morgret, L.; Shull, K. R. *Macromolecules* **2009**, *42*, 7605–7615.

(8) Jovanovic, R.; Dubé, M. A. *J. Macromol. Sci., Part C: Polym. Rev.* **2004**, *C44* (1), 1–51.

(9) Joanicot, M.; Wong, K.; Cabane, B. *Macromolecules* **1996**, *29*, 4976–4984.

(10) Keddie, J. L. *Mater. Sci. Eng., R* **1997**, *21* (3), 101–170.

(11) Landfester, K. *Macromol. Rapid Commun.* **2001**, *22* (12), 896–936.

(12) Asua, J. M. *Prog. Polym. Sci.* **2002**, *27* (7), 1283–1346.

(13) El-Aasser, M. S.; Sudol, E. D. In *Miniemulsions: Overview of Research and Applications*, Roy W Tess Award in Coatings Symposium, Boston, MA, Aug, 2002; Boston, MA, 2002; pp 21−31.

(14) Schork, F. J.; Luo, Y. W.; Smulders, W.; Russum, J. P.; Butte, A.; Fontenot, K. Miniemulsion polymerization. In *Polymer Particles*, 2005; Vol. 175, pp 129−255.

(15) Hegedus, C. R.; Kloiber, K. A. *J. Coat. Technol.* **1996**, *68* (860), 39–&.

(16) Hirose, M.; Kadowaki, F.; Zhou, J. H. *Prog. Org. Coat.* **1997**, *31* (1−2), 157–169.

(17) Kukanja, D.; Golob, J.; Zupancic-Vlant, A.; Kranjc, M. *J. Appl. Polym. Sci.* **2000**, *78*, 67–80.

(18) Wang, C.; Chu, F.; Graillat, C.; Guyot, A. *Polym. React. Eng.* **2003**, *11* (3), 541–562.

(19) Wang, C.; Chu, F.; Graillat, C.; Guyot, A.; Gauthier, C. *Polym. Adv. Technol.* **2005**, *16*, 139–145.

(20) Wang, C.; Chu, F.; Graillat, C.; Guyot, A.; Gauthier, C.; Chapel, J. P. *Polymer* **2005**, *46*, 1113–1124.

(21) Wang, C.; Chu, F.; Guyot, A. *J. Dispersion Sci. Technol.* **2006**, *27* (3), 325–330.

(22) Wang, C. P.; Chu, F. X.; Jin, L. W.; Lin, M. T.; Xu, Y. Z.; Guyot, A. *Polym. Adv. Technol.* **2009**, *20* (3), 319–326.

(23) Li, M.; Daniel, E. S.; Dimonie, V.; Sudol, E. D.; El-Aasser, M. S. *Macromolecules* **2005**, *38*, 4183–4192.

(24) Hirose, M.; Zhou, J. H.; Nagai, K. *Prog. Org. Coat.* **2000**, *38* (1), 27–34.

(25) Sebenik, U.; Krajnc, M. *J. Polym. Sci., Part A: Polym. Chem.* **2005**, *43*, 4050–4069.

(26) Deplace, F.; Rabjohns, M. A.; Yamaguchi, T.; Foster, A. B.; Carelli, C.; Lei, C. H.; Ouzineb, K.; Keddie, J. L.; Lovell, P. A.; Creton, C. *Soft Matter* **2009**, *5*, 1440–1447.

(27) Zosel, A. *Colloid Polym. Sci.* **1985**, *263*, 541–553.

(28) Lakrout, H.; Sergot, P.; Creton, C. *J. Adhes.* **1999**, *69* (3/4), 307–359.

(29) Zosel, A. *J. Adhes.* **1989**, *30* (1−4), 135–149.

(30) Deplace, F.; Carelli, C.; Mariot, S.; Retsos, H.; Chateauminois, A.; Ouzineb, K.; Creton, C. *J. Adhes.* **2009**, *85*, 18–54.

(31) Yamaguchi, T.; Koike, K.; Doi, M. *Europhys. Lett.* **2007**, *77* (6).

(32) Turreda, L. D.; Sonoda, H.; Hatano, Y.; Mizumachi, H. *Holzforschung* **1991**, *45* (6), 461–466.

(33) Tse, M. F.; Jacob, L. *J. Adhes.* **1996**, *56*, 79–95.

(34) Chang, E. P. *J. Adhes.* **1991**, *34*, 189–200.

(35) Yang, H. W. H.; Chang, E. P. *Trends Polym. Sci.* **1997**, *5* (11), 380–384.

(36) Creton, C.; Leibler, L. *J. Polym. Sci., Part B: Polym. Phys.* **1996**, *34*, 545–554.

(37) Glassmaker, N. J.; Hui, C. Y.; Yamaguchi, T.; Creton, C. *Eur. Phys. J. E* **2008**, *25* (3), 253–266.

(38) Good, R. J. *J. Adhes.* **1972**, *4*, 133–154.

(39) Verdier, C.; Piau, J. M. *J. Polym. Sci., Part B: Polym. Phys.* **2003**, *41* (23), 3139–3149.

(40) Roos, A.; Creton, C. *Macromolecules* **2005**, *38* (18), 7807–7818.

(41) Rubinstein, M.; Panyukov, S. *Macromolecules* **2002**, *35*, 6670–6886.

(42) Edwards, S. F.; Vilgis, T. A. *Rep. Prog. Phys.* **1988**, *51* (2), 243–297.

(43) Grassl, B.; Alb, A. M.; Reed, W. F. *Macromol. Chem. Phys.* **2001**, *202* (12), 2518–2524.

(44) Lopez, A.; Degrandi, E.; Creton, C.; Asua, J. M. Simultaneous Free Radical and Addition Miniemulsion Polymerization: Effect of the Diol on the Microstructure of Polyurethane-Acrylic Pressure Sensitive Adhesives. *Polymer*, **2010**, submitted for publication.

(45) Florez, S.; Munoz, M. E.; Santamaria, A. *Macromol. Mater. Eng.* **2006**, *291*, 1194–1200.

(46) Tong, J. D.; Jerome, R. *Polymer* **2000**, *41* (7), 2499–2510.

(47) Moghbeli, M. R.; Zamir, S. M.; Molaee, B. *J. Appl. Polym. Sci.* **2008**, *108* (1), 606–613.

(48) Wang, C.; Chu, F.; Guyot, A.; Gauthier, C.; Boisson, F. *J. Appl. Polym. Sci.* **2006**, *101*, 3927–3941.

(49) Bellamine, A.; Degrandi, E.; Gerst, M.; Stark, R.; Beyers, C.; Creton, C. *Macromol. Mater. Eng.* **2010**, *296* (1), 31–41.

(50) For 15 wt % of PU, the stress does not go back to zero for technical reasons. The maximum scale of the extensometer measuring the probe displacement is 5 mm. For the 15% sample, when the probe reaches 5 mm, fibrils joining the probe and the adhesive layer remain. These fibrils neither fail for a high deformation nor after waiting a long time. They can break cohesively or adhesively when the test is stopped and the probe is removed manually.